Published in final edited form as:
Biomaterials. 2010 May ; 31(14): 3997–4008. doi:10.1016/j.biomaterials.2010.01.144.

The Effect of Incorporation of SDF-1α into PLGA Scaffolds on Stem Cell Recruitment and the Inflammatory Response

Paul Thevenot, M.Sc., **Ashwin Nair, M.Sc.**, **Jinhui Shen, M.D.**, **Parisa Lotfi, M.Sc.**, **Cheng Yu Ko, M.Sc.**, and **Liping Tang, Ph.D***
Bioengineering Department, University of Texas at Arlington, PO Box 19138, Arlington, TX 76019-0138

Abstract

Despite significant advances in the understanding of tissue responses to biomaterials, most implants are still plagued by inflammatory responses which can lead to fibrotic encapsulation. This is of dire consequence in tissue engineering, where seeded cells and bioactive components are separated from the native tissue, limiting the regenerative potential of the design. Additionally, these interactions prevent desired tissue integration and angiogenesis, preventing functionality of the design. Recent evidence supports that mesenchymal stem cells (MSC) and hematopoietic stem cells (HSC) can have beneficial effects which alter the inflammatory responses and improve healing. The purpose of this study was to examine whether stem cells could be targeted to the site of biomaterial implantation and whether increasing local stem cell responses could improve the tissue response to PLGA scaffold implants. Through incorporation of SDF-1α through factor adsorption and mini-osmotic pump delivery, the host-derived stem cell response can be improved resulting in 3X increase in stem cell populations at the interface for up to 2 weeks. These interactions were found to significantly alter the acute mast cell responses, reducing the number of mast cells and degranulated mast cells near the scaffold implants. This led to subsequent downstream reduction in the inflammatory cell responses, and through altered mast cell activation and stem cell participation, increased angiogenesis and decreased fibrotic responses to the scaffold implants. These results support that enhanced recruitment of autologous stem cells can improve the tissue responses to biomaterial implants through modifying/bypassing inflammatory cell responses and jumpstarting stem cell participation in healing at the implant interface.

Keywords

mesenchymal stem cell; hematopoietic stem cells; inflammation; angiogenesis; scaffold; biocompatibility

1. Introduction

Tissue engineering is a discipline of regenerative medicine for which the basic goal is to provide a temporary matrix to replace extracellular matrix upon which cells can be seeded and synthesize new ECM as the temporary matrix degrades [1]. Despite considerable advancements

*Correspondence to Liping Tang, Ph.D., Bioengineering Department, University of Texas at, Arlington, P.O. Box 19138, Arlington, TX 76019-0138. fax: 817-272-2251; ltang@uta.edu.

in biomaterial synthesis and modification techniques, most TE scaffolds, both acellular and seeded, elicit fibrotic reactions resulting in encapsulation of the implant. Such fibrotic reactions often hinder the vascularization of scaffold implants which leads to a bare necrotic core in cell seeded constructs [2]. It is generally believed that controlled wound healing and angiogenesis are critical to the short-term survival/behavior and long-term functionality/integration of seeded cells [3]. For cells to survive in vivo, it has been estimated that cells must reside within 200μm of a capillary bed [4]. Indeed, many studies have shown that cells seeded below the scaffold exterior surface do not survive and require some degree of prevascularization in vitro to survive in vivo [5]. In a recent investigation, mesenchymal stem cells (MSC) seeded by various methods onto scaffolds implanted subcutaneously showed the majority of cells (~75% depending on seeding method) die within 2 weeks [6]. To improve cell survival and functionality, better approaches to reduce fibrotic tissue formation associated with biomaterial implants is urgently required.

To minimize fibrotic reactions to implants, the majority of the past and current research focuses on reducing cell:material interactions. However, the major drawback of this approach is that scaffold implants induce very little short term cell infiltration, resulting in cell buildup at the tissue:material interface, inducing a significant fibrotic response effectively walling off the biomaterial implant. Thus the ability to control the extent and duration of inflammatory response has emerged as a critical design parameter which may ultimately dictate the success of TE designs in vivo [7]. However, traditional anti-inflammatory treatments, such as the use of dexamethasone, may impair wound healing and tissue regeneration [8]. There is still a need for the development of novel treatment to reduce fibrotic reactions while to promote tissue regeneration and angiogenesis.

Due to their unique pluripotency and regenerative properties, stem cells have been intensively studied as powerful therapeutic tools for a variety of diseases and conditions. Recently, groups have focused on the beneficial effects of stem cell participation in inflammation, with mounting evidence supporting improved wound healing outcomes possibly through physical and paracrine influences [9]. Following induced injury, local delivery of stem cells has been shown to reduce inflammation, angiogenesis, and to improve function outcomes in many different models [10]. However most of these models employ transplanted exogenous stem cells. These approaches are complicated by many limitations due to cell sources, expense to achieve sufficient cells for a dose response, xenogenic components necessary to expand the cells, control over the functionality and behavior of these cells, and potential host vs. graft responses. In addition, transplanted cultured and differentiated stem cells may not respond to the physiological microenvironmental stimuli like circulating stem cells [11]. Since stem cells are recruited to the injury sites to participate in wound healing and tissue regeneration, it is our belief that the complications associated with biomaterial scaffold implantation may be reduced or even eliminated if autologous stem cells are purposefully recruited to the tissue scaffold and implantation sites.

Recently, studies have uncovered that the implantation of foreign bodies, including biomaterials, may prompt the recruitment and local engraftment of autologous stem cells [12]. The recruitment of autologous stem cells may be substantially enhanced with localized release of stem cell chemokines. We are specifically interested in stromal derived factor-1 alpha (SDF-1α), since many prior publications have shown that SDF-1α is critical to hematopoietic stem cell (HSC), and possibly MSC migration, and can be used to target stem cells to a desired site within the body [13]. Coincidentally, SDF-1α is also involved in the recruitment of inflammatory cells and other types of stem cells including tissue committed stem cells [14]. Based on these observations, we hypothesized that localized release of SDF-1α may facilitate the recruitment of autologous stem cells to tissue engineering scaffolds and subsequently enhance tissue regeneration.

To test the hypothesis, degradable scaffolds capable of locally releasing SDF-1α via physical adsorption (short term release) or osmotic pumps (long term release), were produced and then implanted in the subcutaneous space of mice. Our objectives were to (1) monitor the effects of SDF-1α on stem cell recruitment, (2) quantify the effects of increased host stem cell responses on the inflammatory response, and (3) examine long term effects on fibrotic and angiogenic processes on SDF-1α supplemented implants.

2. Materials and methods

2.1. PLGA Salt-Leached Scaffold Fabrication

PLGA salt leached scaffolds were fabricated following an established procedure [15]. Briefly, PLGA (75:25) (113kDa, Medisorb Inc., Birmingham, AL) was dissolved in dichloromethane at 10% (w/v). NaCl (porogen weight fraction of 90%, sieved between 100–250μm) was then mixed evenly with PLGA solution and then air dried under a fume hood. After 72 hours, the scaffold was placed under vacuum to complete solvent evaporation overnight. For the salt leaching process, all scaffolds were submersed in distilled water and placed on an orbital shaker at 100RPM. The water was changed every 30 minutes at room temperature until chlorides could not be detected by addition of 0.1M silver nitrate. After salt-leaching, porous scaffolds were cut into 5 × 5 × 5 mm cubes, dried and disinfected by submersion in 70% ethanol overnight. After 24 hours, the ethanol is exchanged by submerging the scaffolds in PBS and orbital shaking 3 times for 5–10 minutes.

2.2. In Vitro Model of Stem Cell Homing and Engraftment

To examine the site directed homing capability of the scaffold:SDF-1α system, a homing and engraftment transwell model was developed. Briefly, scaffolds were injected with 50 ul (approximate to the scaffold retention volume) of SDF-1α (Prospec-Tany TechnoGene, Rehovot, Israel) at 1 μg/mL or PBS (as control). Our preliminary studies have found that such method provided the release of SDF-1α for approximately 5 days [16]. Scaffolds were then cut to fit beside transwell inserts (3 × 3 × 1 mm) in the lower chamber of 8μm pore membranes of 24-well plates (Corning Costar, Corning, NY). Primary murine bone marrow derived MSC were obtained as previously described [17]. Briefly, the femur and tibia bone marrow of 6–8wk old Balb/c was flushed with DMEM containing 20% FBS and plated into 75cm^2 tissue culture flasks. Non-adherent cells were removed from the culture at day 3, with fresh media supplied at 50% with the remaining 50% conditioned media from which non-adherent cells were removed. Media was continually renewed every 3 days with subculture upon confluence up to the fourth passage. At fourth passage, MSC were verified for phenotype by positive stain for SSEA-4 and negative expression of CD45 (Santa Cruz Biotech, Santa Cruz, CA). Prior to scaffold placement, bone marrow derived MSC were labeled with the cell tracer dye CDFA-SE (Invitrogen) and seeded onto transwell inserts. The MSC expansion media was removed and replaced with fresh media in the upper and lower chambers. SDF-1α was allowed to release from the scaffolds into the lower chamber, and the percentage of transmigrated MSC from top chamber to bottom chamber was quantified. Briefly membranes were scraped on the upper side to remove adherent cells, detached from insert, and H&E stained to visualize and quantify cell migration to the lower side of the membrane. To verify cell engraftment, scaffolds were removed from the bottom wells, fixed in cold methanol, and visualized via CFDA-SE staining as previously described [15].

2.3. Animal Implantation Model and SDF-1α Delivery to Implanted Scaffolds

Scaffolds were implanted in the subcutaneous cavity of Balb/C mice as established in early studies [18]. For implantation, mice were anesthetized with isofluorane and the incision site marked and disinfected with 70% ethanol. A vertical incision was made down the midline of the back. Control PLGA scaffolds were implanted to one side of the incision and tucked

subcutaneous away from the incision. For short term study, the scaffolds were injected with 50 μL (approximate to the scaffold retention volume) of SDF-1α at 1 μg/mL or PBS (as control). To achieve long term release, 2 week delivery mini-osmotic pumps (Alzet Model 1002, Alza Corporation, Palo Alsot, CA) delivering SDF-1α at a rate of 0.25ng/hour were inserted into the center of the scaffold (5 × 5 × 5 mm) via a polyvinyl chloride catheter (Alzet, Durect Corporation, Cupertino, CA). The configuration was selected to allow for uniform diffusion of the chemokine through the scaffold into the surrounding tissue space. SDF-1α-loaded scaffolds and controls were placed contra-lateral for short term studies. For long-term studies, SDF-1α pumps and saline control pumps were placed into individual animals.

At the end of the experiments, animals were sacrificed by CO_2 inhalation and implants and surrounding tissue was embedded in optimal cutting temperature (OCT) compound (Tissue-Tek; Sakura Finetek, Torrance, CA) and frozen sectioned for histological and immunohistochemical staining and protein array analyses.

2.4. Histology, immunohistochemistry and image analyses

To determine the extent of fibrotic responses to scaffold implants, some slides were stained with Hematoxylin and Eosin Y (H&E stain, Sigma, St. Louis, MO) according to the manufacturer's instruction. Toluidine Blue (Sigma, St. Louis, MO) staining was carried out on some slides to visualize mast cell density and activation state from images taken of the material: tissue interface [18]. Mast cells were considered degranulated if there was an extensive dispersion of more than 15 extruded vesicles localized near the cell or when there was an extensive loss of granule staining. Masson Trichrome stain (Sigma. St. Louis, MO) was also carried out as described earlier to assess the extent of collagen deposition [19]. A series of immunohistochemical stains were done to determine the types of recruited cells. Specifically, $SSEA4^+/CD45^-$ [20] was used to identify MSC. HSC were detected by expression of the markers c-kit, CD34, or Sca-1. Inflammatory cells were identified by $CD11b^+$ expression [21]. MOMA-2 antibody (Serotec, Oxoford, UK) was used to identify macrophage composition in the tissue response to 2 week scaffold implants. The presence of endothelial progenitor cells was assessed by co-expression of CD34 and CD133 [22]. Antibody staining was visualized by immunofluorescence with FITC and Texas Red conjungated secondary antibodies (ProSci, Poway, CA). Staining with 4′,6-diamino-2-phenylindole dihydrochrolide (DAPI) (Invitrogen; Carlsbad, CA) was used to stain cell nuclei. Unless otherwise stated all primary and second antibodies used in this work were purchased from Santa Cruz Biotech (Santa Cruz, CA) and stained according to manufacturer's recommendations. Stained sections were visualized using a Leica microscope and imaged with a CCD camera (Retiga EXi, Qimaging, Surrey BC, Canada). The measurements of tissue thickness and cell densities at the material:tissue interface were then performed in Image J [23]. Measurement of density and thickness were collected from the average of multiple counts taken from H&E stained cross-sections of the scaffold and surrounding tissue, with images captured on the skin side of the biomaterial interface for each sample (n=4). For these calculations, thickness of interface capsules was measured from the biomaterial perpendicular where the capsular tissue met native healthy tissue. Density was measured in random areas of the capsule extending from biomaterial to native healthy tissue with the area held constant for all treatment group quantifications. The percentage of fibroblasts in the interface was estimated for population plots through quantification of spindle shaped cells near the implant in the capsular interface surrounding the scaffolds. Collagen deposition was visualized around the implants by Masson Trichrome staining.

The engraftment of MSC from the blood was quantified using an in vivo model of stem cell mobilization. Briefly, Balb/c mice were implanted with either control or SDF-1α supplemented scaffolds using procedures described previously for longitudinal SDF-1α supplemented

scaffold studies. To minimize interference from the incision site and maximize the distance between scaffold treatment groups, scaffolds were placed vertical along the back of the mice opposite to the incision site on the opposite side of the mouse. The configuration of implants with respect to upper verses lower position on the back was randomized to account for the effects of implant placement. Bone marrow-derived MSC were recovered from Balb/c mice and purified using plastic adhesion and verified for SSEA-4^+ $CD45^-$ as outline for in vitro transwell studies. Cells were loaded with Xsite 761 (Carestream Health, New Haven CT) at a concentration of 2μM for a period of 3hrs. After detaching MSC, uptake was assessed by NIR fluorescence intensity (excitation-761nm emission-789nm) using Kodak FX Pro imaging system (Carestream). After implantation for 2 days, a 100μL PBS solution containing 1×10^6 bone marrow-derived MSC was injected into the tail vein. The location of MSC cells in relation to implanted scaffolds was monitored and fluorescent intensity measurements taken over the region of interest daily until signal subsided.

2.5. Inflammatory Protein Array

The profile of inflammatory protein production by implant-associated cells was determined using mouse cytokine antibody array III (Raybiotech, Norcros, GA) compared with control implants (n=3). Briefly, 30 slices of tissue sections from both control and treated groups were incubated with lysis buffer in −80°C 30 minutes followed by 30 minutes at room temperature for 3 cycles to extract proteins produced by cells adjacent to the implants. The protein concentrations in each sample were then determined using bicinchoninic acid (BCA) assay (Thermo Fisher Scientific Pierce Protein Research Products, Rockford, IL) as recommended by the manufacturer. For the antibody array, 50 μg of each protein sample was used in the mouse cytokine antibody array III following manufacture's instruction. Finally, the slides were subjected to image analysis by Axon GenePix 4000B microarray scanner (Molecular Devices, Sunnyvale, CA) using Cy3 channel. The ratio of relative expression of SDF-1α treated scaffolds was calculated after subtraction of the background intensity and comparison with untreated controls. The fluorescence ratio for each spot was further processed to identify the species of up-regulated and down-regulated cytokines/growth factors.

2.6. Statistical Analysis

GraphPad (La Jolla, CA) was used for all statistical operations. Difference in group means was assessed using ANOVA (P=0.05). Differences which registered $p < 0.05$ were considered significant.

3. Results

3.1. Effects of SDF-1α on MSC homing in vitro

The ability of SDF-1α to induce chemotaxis in vitro was tested using a transwell system as depicted (Figure 1A). Indeed, SDF-1α release from the PLGA scaffold was able to induce cell migration across the transwell membrane (Figure 1B). We find that both the addition and interval of SDF-1α correlate to the degree of migrated MSC (Figure 1C). To further characterize this response, we monitored the SDF-1α releasing scaffolds for cell adherence on the scaffolds using CFDA-SE cell tracing. Indeed, MSC were found to transverse the membrane and engraft on the surface of the PLGA salt-leached scaffolds placed in the lower chamber. Engrafted cells obtained an adherent morphology on the scaffold as shown (Figure 1D).

3.2. Effects of SDF-1α on stem cell recruitment in vivo

We next sought to determine whether scaffold treatment with SDF-1α could result in measurable alterations in the stem cell response to subcutaneous implant scaffolds. Indeed, after implantation for one week, SDF-1α soaked scaffolds were found to have attracted a

substantially larger number of MSC compared with control scaffolds (Figure 2A & 2B). Specifically, the density of MSC surrounding SDF-1α soaked scaffolds is about 3 times higher than those associated with control scaffolds at both 3-day and 7-day time points (Figure 2C). In addition to an increase in interface density, we also find enhanced (2-fold increase) density of MSC within the matrix of SDF-1α soaked scaffold compared with control scaffolds at day 7 (Figure 2D).

In order to establish whether SDF-1α release was effective at mobilizing MSC from the circulation, an in vivo imaging experiment with NIR labeled MSC was performed. Indeed at 48hrs after injection (3 days implantation), SDF-1α supplemented scaffolds were able to attract and engraft tail vein supplemented MSC based on co-localization of NIR fluorescent signal over the region of scaffold implantation (Figure 2E).

Since SDF-1α treatment improved MSC responses, and given precedent for SDF-1α mediated HSC chemotactic responses, we quantified the time-scale recruitment of c-kit$^+$ HSC to the site of scaffold implantation using fluorescent IHC. Consistent with MSC responses, we observe a progressive increase in c-kit$^+$ cell density over the course of the implantation study (Figure 3A & 3B). Quantification of these responses on basis of cell density reveals significant increase at time points of 3 days and 7 days compared to unmodified scaffolds (Figure 3C). To further investigate this response, we quantified the density of other common markers used to identify HSC, namely CD34 and Sca-1, between SDF-1α treatment and control groups. In accordance with c-kit results, we observe a significant week 1 increase in the density of both CD34 and Sca-1 positive cells with respect to control. Quantification reveals a greater than 2-fold increase consistent with c-kit$^+$ cells at the same time point (Figure 3D).

3.3. Inflammatory cell and foreign body responses

We next sought to examine whether these interactions had measurable effects on the inflammatory response. Given that our current understanding of the mechanism of foreign body reactions suggests that mast cell activation and its products effect the initial recruitment of inflammatory cells, it is possible that SDF-1α release may also affect mast cell reactions. To test the hypothesis, the densities of mast cells surrounding both scaffold groups were examined at day 3, the time point associated with the first measurable increase in MSC responses. As expected, control scaffolds prompted the recruitment and degranulation of large numbers of mast cells (Figure 4A). We also found that SDF-1α soaked scaffolds elicited substantially less accumulation of mast cells (mostly non-activated) compared with controls (Figure 4B). Quantification of density in the reaction tissue reveals an 84% reduction in mast cell density around the treated implants (Figure 4C). Downstream monitoring of mast cell responses in short-term release implants yielded significant differences in the mast cell response up to 6 weeks, though less substantial than that observed at Day 3.

Since inflammatory cells are the major component of the fibrotic capsule surrounding biomaterial implants, and their participation may be linked to mast cell activation, we hypothesized that altering the stem cell and mast cell responses may reduce the accumulation of inflammatory cells (CD11b$^+$ cells) at the implant interface. Indeed, control implants were found to have a thick, dense band of CD11b$^+$ cells (Figure 4D) while SDF-1α soaked implants have a substantially reduced density of inflammatory cells (Figure 4E). By quantifying the cell density, we find that SDF-1α soaked implants elicited little influence on inflammatory cell recruitment at day 3. However, SDF-1α release profoundly reduced inflammatory cell accumulation 3-fold less than control implants after one week of implantation (Figure 4F).

Since inflammatory cells, especially CD11b$^+$ macrophages, at the interface participate in the formation of granulation tissue and subsequent fibroblast interactions, we examined the influence of SDF-1α release on tissue responses associated with scaffold implant at 1 week

(Figure 5). First, as anticipated, we found that SDF-1α soaked scaffolds exert substantially less inflammatory cell infiltration and granulation tissue formation than control scaffolds at day 7 (Figure 5A & 5B). Treated implants have a 2 fold reduction in thickness of the inflammatory infiltrate (Figure 5C) and a ~1 fold decrease in cell density (Figure 5D) compared to control implants. Based on the cell density calculated in H&E images, we finally quantified the cellular composition at the interface between treatment groups (Figure 5E). In control scaffolds at week 1, the scaffold interface was composed of approximately 75% inflammatory ($CD11b^+$) cells and fibroblasts (residual spindle shaped cells of the interface which do not stain positive for the specified marker set). In contrast, implants treated with SDF-1α prior to implantation leads to a week 1 interface with approximately 75% composition of MSC and HSC.

3.4. SDF-1α on inflammatory cell and stem cell responses

Since physical adsorption leads to early burst release, we investigated an additional supplementation strategy aiming to investigate downstream delivery of SDF-1α during the period immediately prior to increased stem cell presence at the implantation site. Specifically, untreated scaffolds were implanted for 3 days, after which a 100μL SDF-1α solution at 100ng/mL (labeled as D3) was injected into the center of the scaffold in vivo. Explant analysis at Day 7 reveals unexpectedly that delayed deliver leads to an intermediate response compared to control and scaffolds treated with SDF-1α prior to implantation (labeled as D0) (Figure 6A–6B). SDF-1α treatment at Day 0 and Day 3 resulted in significant increase in MSC engraftment at the scaffold interface compared to no treatment (Figure 6A), though differences between SDF-1α treatment intervals was not significant. However, delaying the chemokine until Day 3 resulted in an intermediate $CD11b^+$ inflammatory cell response, significantly less than control yet greater than treatment prior to implantation (Figure 6B).

3.5. Effects of sustained delivery of SDF-1α

To analyze cellular and tissue response parameters beyond 7 days, scaffolds were implanted with either saline mini-osmotic pumps as control or pumps delivering SDF-1α at 100ng/mL for 2 weeks. Similar to pre-implantation soaking, we observe an altered mast cell response around the scaffold implants after 2 weeks. In the absence of SDF-1α, control scaffolds we surrounded by degranulated mast cells (Figure 7A). However, the SDF-1α pump implants had a reduced total presence of mast cells and very few degraulated mast cells (Figure 7B). These differences were quantified as a 59% reduction in mast cell response and a 75% decrease in degranulated mast cells at day 14 (Figure 7C) with respect to control implants.

Given that current models of biomaterial-mediated inflammatory responses suggest long-term effect of macrophages on foreign body reactions, we used antibodies specific to murine macrophages as an additional comparison against the more general $CD11b^+$ marker which may include other cell types such as neutrophils. As previously shown in inflammatory cell quantifications for mini-osmotic pump interfaces, the density of $CD11b^+$ cells at the implant interfaces is much higher in control scaffold (Figure 7D) compared to SDF-1α pumps (Figure 7E). As expected, this trend is also apparent with regard to macrophages, as control scaffolds have a higher density of macrophages surrounding implants (Figure 7F) compared to SDF-1α scaffolds (Figure 7G) which have a lower density with distribution restricted to small pockets long the skin side of the scaffold interface.

We next examined the relationship which emerged in soaked studies between MSC responses and $CD11b^+$ inflammatory cell responses. First, as expected, the engraftment of MSC was significantly higher in SDF-1α treated scaffolds as opposed to controls. Interestingly, the same stem cell: inflammatory cell trend was present in the pump implants, where MSC density is elevated with reduced inflammatory cell density with respect to control at 2 weeks (Figure

7H). In addition, comparison of the inflammatory cell density between control saline and SDF-1α mini-osmotic pumps reveals a significant decrease with respect to untreated control.

Histological analyses show onset of granulation tissue in control implants with a multi-cell thick granulocyte and fibroblast layer forming between the implants and surrounding tissue. In contrast, SDF-1α pump implants have reduced cell density and a less organized tissue capsule around the implants. We hypothesized that altered inflammatory cell responses at the interface may be affecting the deposition of collagen around the implants at 2 weeks as part of the initiation of the fibrotic response. Control scaffolds show a characteristic 2 week fibrotic response with a thick layer of collagen deposition surround the scaffold implants (Figure 7I). In contrast, SDF-1α treated scaffolds had a very thin layer of collagen formation compared with controls (Figure 7J). Interestingly, we also found a 35% reduction in capsule thickness (data not shown) and 60% reduction in capsular cell density (Figure 7K) in SDF-1α pump connected implants.

As previously mentioned, 2 week control implants were characterized by a thick encapsulating cell layer as part of the developing fibrotic tissue around the scaffold implants. Interestingly, in conjunction with the absence of this multi-cell thick granulation tissue, SDF-1α pump implants also had many vessels organized throughout the interface between the native tissue and the scaffold (Figure 8A). Notably, this vessel formation in the interface at 2 weeks was less evident in control scaffolds. However, an aim of biomaterial scaffold integration in tissue engineering is to induce vessel formation not only at the interface, but within the scaffold to initiate cell infiltration and mineralization. The difference in vessel formation inside the scaffold matrix was therefore quantified as a measure of enhanced intra-scaffold angiogenesis. Since an increased number of vessels at the interface were observed in the treatment group, sections were stained with CD31 to verify endothelial cell phenotype. For both treatment conditions, vessels identified in H&E staining were confirmed in subsequent sections as expressing CD31. SDF-1α pump samples showed over a 3-fold increase in the number of vessels within the scaffold matrix accompanied by a deeper vessel penetration, compared to control scaffolds initiating non-uniform vessel formation restricted to the edges of the scaffold (Figure 8B).

This led us to consider that the differences in $CD11b^+$ cell responses and macrophage responses may be due to altered activation of the macrophages, leading to macrophage participation in other aspects of wound healing. Recent evidence suggests that bone marrow-derived macrophages participate in angiogenesis and lymphogenesis at the sites of inflammation [24, 25]. We thus investigated the potential role of bone marrow-derived macrophages in scaffold-associated tissue responses based on the co-expression of $CD11b^+$ $VEGFR\text{-}1^+$ (mononuclear myeloid cells with the capacity to induce proangiogenic activities) [24] and $CD11b^+$ $LYVE\text{-}1^+$ (macrophages which participate in lymphangiogenesis in healing tissue) [25]. Interestingly, we observe little participation of $CD11b^+$ $VEGFR1^+$ cells in control implants (Figure 8C). However, at sites of vessel formation in SDF-1α treated implants we observe co-staining identifying these cells in the presence of budding vessels (Figure 8C). In addition, we see a few $CD11b^+$ $LYVE\text{-}1^+$ cells in control scaffolds (Figure 8D), with these cells expressed at specific locations throughout the interface in SDF-1α treated implants (Figure 8D). This suggests that inflammatory cells have been primed to participate in integrating host tissue with implant to a much higher degree than that observed in untreated implants.

Given the pluripotency of induced host-derived stem cells engrafted at the interface based on marker expression in SDF-1α treated scaffolds, we hypothesized that these cells may be participating in the observed vessel budding at the interface and within scaffold implants. Using 2 week SDF-1α pump implants from which we observe improved angiogenesis in histological analysis, we additionally analyzed interfaces for endothelial progenitor cell (EPC) engraftment.

Indeed both within the cross-section (Figure 8E) and at the interface of SDF-1α scaffolds (Figure 8F) we observe vessel-like formations with cells staining $CD34^+$ $CD133^+$ consistent with an EPC phenotype.

3.6. Effect of SDF-1α on inflammatory cytokine profile

Given that studies suggested a complex relationship between inflammatory cells, fibroblasts, and granulation tissue and subsequent fibrosis responses, and SDF-1α release appears to alter these processes, we determined the characteristics of the local cytokine/chemokine environment using protein micro-arrays. In agreement with histological evaluation, we have found that the presence of SDF-1α reduced the production of a variety of inflammatory cytokines and chemokines, including IL-13, IL-3Rβ, IL-4, IL-5, IL-9, Leptin R, L-selectin, Lymphotactin, MIP-3α/β, TCA3/CCL1, and TNF-α (Table 1). Specifically, in support of altered mast cell responses we find the mast cell growth factors IL-3, IL-4, and IL-9 are substantially downregulated. It should also be noted that the treatment of SDF-1α profoundly increased the release of several inflammatory cytokines, including GCSF, GM-CSF, IL-6, KC/CXCL1, MIP-1 α/CCL3, MIP-2/CXCL1, PF-4/CXCL4, sTNF RII/CD120b, TARC/CCL17, and TIMP-1.

Interestingly, the treatment of SDF-1α was found to reduce the production of several pro-fibrotic cytokines, including IL-13, PF-4/CXCL4, and TIMP-1 (Table 1). In addition, in support of SDF-mediated angiogenic responses, we observe high upregulation of many cytokines related to angiogenic processes, including IGFBP-3, VEGF, and GM-CSF. Finally, treatment with SDF-1α appears to have significant influence on many other factors, including G-CSF, VEGF, and CXCL16, related to stem cell mobilization and homing. Surprisingly, the levels of tissue expression for SDF-1α are only slightly higher (< 2X increase) in the tissue and scaffold infiltrating cells of SDF-1α treated implants.

Most convincing of these cytokine comparisons is the uniform decrease in cytokines associated with macrophage activation in SDF-1α scaffolds. Cytokines involved in macrophage activation including CD40 (>2X), TNF-α (>2), IFN-γ (>1.5), IL-4 (>2), IL-10 (>2), IL-13 (>5), IL-1β (>1.2), and Lymphotactin (>3) are decrease in SDF-1α scaffolds with respect to control (Table 1).

4. Discussion

In this study we investigated whether host derived stem cells could be triggered to home and engraft to scaffold implants to improve biomaterial-mediated tissue responses through treatment with a stem cell chemokine, SDF-1α. In addition, we hypothesized that this process, if successful, may alter inflammatory and fibrotic outcomes. Although SDF-1α has shown stem cell chemotactic properties in vitro [13], it has remained controversial as to whether MSC migration in response to SDF-1α supplementation could be achieved. To test our hypothesis, two different strategies, physical adsorption for short term release and osmotic pump for longer term release, were employed. In support of our assumption, both soaking treatment and pump delivery strategies were found to substantially increase the number of MSC ($SSEA\text{-}4^+$/$CD45^-$) at the implantation site of PLGA scaffolds over the course of the inflammatory response. The extent and length of MSC recruitment depends heavily on the duration of SDF-1α release, since pump implants produced magnified and extended MSC recruitment (Figure 7H) than soaked implants (Figure 2D) which showed little difference in MSC density by the second week. Interestingly, we find that, when administered at day 0, SDF-1α decreases inflammatory cell recruitment and enhances MSCs migration. However, delayed SDF-1α delivery (at day 3), coinciding with the maximal inflammatory response, was found to increase MSC recruitment with no influence on inflammatory responses. These results suggest that SDF-1α can reduce, but not reverse, the inflammatory responses.

In addition to enhanced MSC recruitment, we also observed increased HSC (c-kit$^+$) recruitment to SDF-1α soaked and pump implants (data not shown). HSC, along with MSC, express the receptor CXCR4 [13,14] and are held in the bone marrow through CXCL12-CXCR4 interactions [26]. The gradients of exogenous SDF-1α can lead to the stem cell mobilization and homing [26]. Of interest, with pump implants, the delivery of SDF-1α substantially increases the recruitment of both HSC and MSC at the interface 2 weeks after implantation.

Recently, it was shown that in the absence of injury, the addition of exogenous SDF-1α does not stimulate stem cell migration [27]. Therefore, the inflammatory stimuli due to scaffold implantation in combination with SDF-1α is likely the factor leading to increases beyond those stem cells normally recruited to participate in healing. Many proteins and cytokines are up- or down- regulated by implant-associated tissue exposed to SDF-1α. However, it has yet to be determined by what potential mechanism SDF-1α affects the release of other stem cell chemokines, though we hypothesize that this may be related to altered inflammatory cell responses.

When examining the inflammatory responses to SDF-1α treated scaffolds, we were surprised to find a significant decrease in the density and activation of mast cells accompanied by a downstream decrease in the density of inflammatory (CD11b$^+$) cells in the subcutaneous space around the implant. Since foreign body reactions are initiated by implant-associated mast cell recruitment and activation [18], it is possible that exogenous SDF-1α may directly or indirectly alter the extent of mast cell responses. Indeed, we find that the release of SDF-1α substantially reduces mast cell recruitment and activation. Based on several lines of evidence, we believe that an SDF-1α-mediated reduction of mast cell reactions is likely due to interactions for which a detailed mechanism has not yet been developed. Receptor expression studies have shown that mast cell progenitors express CXCR4 and both mature and progenitor mast cells respond to SDF-1α gradients in vitro [28]. This suggests that CXCR4 may be, at least partially, responsible for mast cell chemotaxis to peripheral tissues [29]. Interestingly however, recent evidence has shown that mast cell treatment with SDF-1α in vitro does not stimulate degranulation, instead selectively stimulates production of IL-8, a mast cell product responsible for initiating neutrophil chemotaxis to the site of inflammation [30]. However, in this study, SDF-1α treatment groups had uniform decrease in CD11b$^+$ cells, which include neutrophils. On the other hand, supplementation of SDF-1α after peak mast cell degranulation, leads to less prominent effects on both host MSC recruitment and the reduction in CD11b$^+$ cells recruited to the implantation site. This suggests a more complex interaction than that observed for SDF-1α in vitro with mast cells. Finally, our protein analysis reveals significant reduction in some of the chemokines, such as CRG-2/CXCL10, TCA-3/CCL1, lymphotactin/CXCL1, leptin receptor, IL-13 which have been shown to trigger mast cell migration [31–33].

The release of SDF-1α was also found to reduce many potent pro-inflammatory cytokines, including TNFa, IL-1β, MIP3α/β, lymphotactin/CXCL1, L-selectin, leptin receptor, IL-9, IL-5, IL-10, Eotaxin-2, CTACK/CCL27, CRG-2/CXCL10, CD30L. Reduction in these cytokines may be responsible for the less destructive inflammatory reactions to scaffold implants [34–36]. Though interestingly, many proinflammatory cytokines which have been linked with stem cell responses and angiogenesis were highly upregulated in SDF-1α treated implants, specifically MIP-2 (120.6X), G-CSF (81.9X), GM-CSF (49.6X), KC (8.6X), MIP-1α (24.4X) and IL-6 (13.5X). In addition, decreases in inflammatory cell engraftment, downregulation in cytokines related to macrophage activation, and the presence of macrophage subsets related angiogenesis and lymphangiogenesis suggests that stem cell interactions and the presence of SDF-1α is likely improving tissue responses to the biomaterial increasing tissue compatibility. These results suggest a potentially complex interaction between SDF-1α, inflammatory responses and stem cell responses.

Since biomaterial-mediated inflammatory responses are often followed with fibrotic tissue reactions [37], it is not surprising to find that SDF-1α treatment reduces not only inflammatory responses but also capsule formation surrounding scaffold implants. It is also possible that SDF-1α treatment may have direct influence on the extent of collagen production. Indeed, our protein array results have shown that IL-13, a cytokine implicated in fibroblast proliferation and collagen production [38], is substantially reduced in tissue exposed to SDF-1α. In addition, our results have shown that SDF-1α treatment reduce Fas Ligand production (3.94x). It should be noted that Fas Ligand appears to be involved in biomaterial-mediated fibrosis [39], and reduced Fas Ligand has been shown to attenuate fibrotic tissue reactions [40]. However, the molecular mechanisms governing SDF-1α-mediated reduction in fibrotic reactions to scaffold implants have yet to be determined.

It is well established that inflammatory products play an essential role in promoting tissue regeneration and angiogenesis. Thus, wound healing responses were impaired when treated with anti-inflammatory agents, such as dexamethasone [41]. However, our results show that SDF-1α can not only reduce inflammatory responses, but also promote tissue regeneration/angiogenesis. Many recent results may shed some lights on this interesting phenomenon. First, it was shown that SDF-1α is involved in the recruitment of $CXCR4^+$ $VEGFR1^+$ hematopoietic progenitors (hemangiocytes) which accelerate revascularization [42]. Second, SDF-1α regulates adhesion of stem cells in vitro and in vivo and promotes differentiation of $CD34^+$ cells to endothelial progenitor cells [43]. Finally, a recent study has shown MSC secrete SDF-1α in culture and that MSC conditioned media concentrated and delivered to a wound site resulted in accelerated wound healing [44].

As previously mentioned, though long-term cytokine delivery is commonly included in tissue engineering designs, little consideration is generally given to the mechanisms governing their observed responses in lieu of long term histological responses. Although various cytokines (including VEGF, PDGF, and FGF) have been incorporated into scaffolds to enhance angiogenesis [4,45,46], these investigations have not explicitly focused on how factors such as these may affect the cascade of the inflammatory and wound healing responses. Here we show that delivery of SDF-1α not only enhanced MSC and HSC migration, but also EPC ($CD34^+$ $CD133^+$) engraftment near the scaffold. In addition, many budding vessel formations identified in H&E stains can be identified through subsequent tissue sections and routinely labeled for CD31, α-SMA, and Laminin, in support of evidence which suggests EPC differentiation in angiogenesis to $CD31^+$ and $\alpha\text{-SMA}^+$ cells [47]. The ability of SDF-1α to generate a pro-angiogenic environment is well supported by the results of a protein assay performed on the scaffolds and surrounding tissue after two weeks of implantation. Though the participation of recruited cells in angiogenesis was not determined, our findings here may provide a novel strategy to improve host responses to biomaterials though recruiting autologous stem cells for tissue regeneration while providing a suitable environment for transplanted cell-containing scaffold with a reduced fibrotic capsule and improved angiogenic environment.

5. Conclusion

In this study, we have provided evidence that delivery of SDF-1α can increase the local recruitment of stem cell populations (both MSC and HSC) to the site of porous scaffold implantation. In addition, SDF-1α treatment also affects the mast cell response resulting in a reduction in mast cell degranulation. These two factors lead to significant downstream alterations in the inflammatory and fibrotic responses, including an altered macrophage response, decreased inflammatory cell accumulation and encapsulation of the scaffolds. This is accompanied by increased wound healing and angiogenesis by decreased collagen deposition encapsulating the scaffold implants and improved vessel formation both at the interface and inside the porous scaffolds. These findings suggest that recruitment of host derived stem cells

may be a viable approach to improve both the tissue response and regenerative potential of tissue engineering scaffolds.

Supplementary Material

Refer to Web version on PubMed Central for supplementary material.

Acknowledgments

This work was supported by NIH grant RO1 EB007271.

References

1. Muschler GF, Nakamoto C, Griffith LG. Engineering principles of clinical cell-based tissue engineering. J Bone Joint Surg Am 2004;86-A(7):1541–1558. [PubMed: 15252108]
2. Silva MM, Cyster LA, Barry JJ, Yang XB, Oreffo RO, Grant DM, et al. The effect of anisotropic architecture on cell and tissue infiltration into tissue engineering scaffolds. Biomaterials 2006;27(35): 5909–5917. [PubMed: 16949666]
3. Jones KS. Effects of biomaterial-induced inflammation on fibrosis and rejection. Semin Immunol 2008;20(2):130–136. [PubMed: 18191409]
4. Laschke MW, Harder Y, Amon M, Martin I, Farhadi J, Ring A, et al. Angiogenesis in tissue engineering: breathing life into constructed tissue substitutes. Tissue Eng 2006;12(8):2093–2104. [PubMed: 16968151]
5. Smith MK, Peters MC, Richardson TP, Garbern JC, Mooney DJ. Locally enhanced angiogenesis promotes transplanted cell survival. Tissue Eng 2004;10(1–2):63–71. [PubMed: 15009931]
6. Seitz S, Ern K, Lamper G, Docheva D, Drosse I, Milz S, et al. Influence of in vitro cultivation on the integration of cell-matrix constructs after subcutaneous implantation. Tissue Eng 2007;13(5):1059–1067. [PubMed: 17394385]
7. Mountziaris PM, Mikos AG. Modulation of the inflammatory response for enhanced bone tissue regeneration. Tissue Eng Part B Rev 2008;14(2):179–186. [PubMed: 18544015]
8. Greco KV, Lara PF, Oliveira-Filho RM, Greco RV, Sudo-Hayashi LS. Lymphatic regeneration across an incisional wound: Inhibition by dexamethasone and aspirin, and acceleration by a micronized purified flavonoid fraction. European Journal of Pharmacology 2006;551(1–3):131–142. [PubMed: 17045986]
9. Copland IB, Lord-Dufour S, Cuerquis J, Coutu D, Annabi B, Wang E, et al. Improved autograft survival of mesenchymal stromal cells by plasminogen activator inhibitor 1 inhibition. Stem Cells 2009;27(2): 467–477. [PubMed: 19338064]
10. Caplan AI. Review: mesenchymal stem cells: cell-based reconstructive therapy in orthopedics. Tissue Eng 2005;11(7–8):1198–1211. [PubMed: 16144456]
11. Mikos AG, Herring SW, Ochareon P, Elisseeff J, Lu HH, Kandel R, et al. Engineering complex tissues. Tissue Eng 2006;12(12):3307–3339. [PubMed: 17518671]
12. Vranken I, De Visscher G, Lebacq A, Verbeken E, Flameng W. The recruitment of primitive Lin(−) Sca-1(+), CD34(+), c-kit(+) and CD271(+) cells during the early intraperitoneal foreign body reaction. Biomaterials 2008;29(7):797–808. [PubMed: 18022690]
13. Sordi V, Malosio ML, Marchesi F, Mercalli A, Melzi R, Giordano T, et al. Bone marrow mesenchymal stem cells express a restricted set of functionally active chemokine receptors capable of promoting migration to pancreatic islets. Blood 2005;106(2):419–427. [PubMed: 15784733]
14. Zhang G, Nakamura Y, Wang X, Hu Q, Suggs LJ, Zhang J. Controlled release of stromal cell-derived factor-1 alpha in situ increases c-kit+ cell homing to the infarcted heart. Tissue Eng 2007;13(8):2063–2071. [PubMed: 17518719]
15. Thevenot P, Nair A, Dey J, Yang J, Tang L. Method to analyze three-dimensional cell distribution and infiltration in degradable scaffolds. Tissue Eng Part C Methods 2008;14(4):319–331. [PubMed: 19055358]

16. Nair A, Thevenot PT, Dey J, Shen J, Sun MW, Yang J, et al. Novel polymeric scaffolds using protein microbubbles as porogen and growth factor carriers. Tissue Eng Part C Methods. 2009
17. Fiorina P, Jurewicz M, Augello A, Vergani A, Dada S, La Rosa S, et al. Immunomodulatory Function of Bone Marrow-Derived Mesenchymal Stem Cells in Experimental Autoimmune Type 1 Diabetes. J Immunol 2009;183(2):993–1004. [PubMed: 19561093]
18. Tang L, Jennings TA, Eaton JW. Mast cells mediate acute inflammatory responses to implanted biomaterials. Proc Natl Acad Sci U S A 1998;95(15):8841–8846. [PubMed: 9671766]
19. Nair A, Zou L, Bhattacharyya D, Timmons RB, Tang L. Species and density of implant surface chemistry affect the extent of foreign body reactions. Langmuir 2008;24(5):2015–2024. [PubMed: 18189430]
20. Gang EJ, Bosnakovski D, Figueiredo CA, Visser JW, Perlingeiro RC. SSEA-4 identifies mesenchymal stem cells from bone marrow. Blood 2007;109(4):1743–1751. [PubMed: 17062733]
21. Solovjov DA, Pluskota E, Plow EF. Distinct roles for the alpha and beta subunits in the functions of integrin alphaMbeta2. J Biol Chem 2005;280(2):1336–1345. [PubMed: 15485828]
22. Yoder MC, Mead LE, Prater D, Krier TR, Mroueh KN, Li F, et al. Redefining endothelial progenitor cells via clonal analysis and hematopoietic stem/progenitor cell principals. Blood 2007;109(5):1801–1809. [PubMed: 17053059]
23. Abramoff, Magelhaes, Ram. Image processing with Image. J Biophotonics Int 2004;11(7):36–42.
24. Grunewald M, Avraham I, Dor Y, Bachar-Lustig E, Itin A, Jung S, et al. VEGF-induced adult neovascularization: recruitment, retention, and role of accessory cells. Cell 2006;124(1):175–189. [PubMed: 16413490]
25. Schledzewski K, Falkowski M, Moldenhauer G, Metharom P, Kzhyshkowska J, Ganss R, et al. Lymphatic endothelium-specific hyaluronan receptor LYVE-1 is expressed by stabilin-1+, F4/80+, CD11b+ macrophages in malignant tumours and wound healing tissue in vivo and in bone marrow cultures in vitro: implications for the assessment of lymphangiogenesis. J Pathol 2006;209(1):67–77. [PubMed: 16482496]
26. Hattori K, Heissig B, Tashiro K, Honjo T, Tateno M, Shieh JH, et al. Plasma elevation of stromal cell-derived factor-1 induces mobilization of mature and immature hematopoietic progenitor and stem cells. Blood 2001;97(11):3354–3360. [PubMed: 11369624]
27. Abbott JD, Huang Y, Liu D, Hickey R, Krause DS, Giordano FJ. Stromal cell-derived factor-1alpha plays a critical role in stem cell recruitment to the heart after myocardial infarction but is not sufficient to induce homing in the absence of injury. Circulation 2004;110(21):3300–3305. [PubMed: 15533866]
28. Godot V, Arock M, Garcia G, Capel F, Flys C, Dy M, et al. H4 histamine receptor mediates optimal migration of mast cell precursors to CXCL12. J Allergy Clin Immunol 2007;120(4):827–834. [PubMed: 17681365]
29. Belot MP, Abdennebi-Najar L, Gaudin F, Lieberherr M, Godot V, Taieb J, et al. Progesterone reduces the migration of mast cells toward the chemokine stromal cell-derived factor-1/CXCL12 with an accompanying decrease in CXCR4 receptors. Am J Physiol Endocrinol Metab 2007;292(5):E1410–1417. [PubMed: 17468394]
30. Lin TJ, Issekutz TB, Marshall JS. Human mast cells transmigrate through human umbilical vein endothelial monolayers and selectively produce IL-8 in response to stromal cell-derived factor-1 alpha. J Immunol 2000;165(1):211–220. [PubMed: 10861054]
31. El-Shazly A, Berger P, Girodet P-O, Ousova O, Fayon M, Vernejoux J-M, et al. Fraktalkine Produced by Airway Smooth Muscle Cells Contributes to Mast Cell Recruitment in Asthma. J Immunol 2006;176(3):1860–1868. [PubMed: 16424217]
32. Shimizu T, Owsianik G, Freichel M, Flockerzi V, Nilius B, Vennekens R. TRPM4 regulates migration of mast cells in mice. Cell Calcium 2009;45(3):226–232. [PubMed: 19046767]
33. Pietrzak A, Misiak-Tloczek A, Brzezinska-Blaszczyk E. Interleukin (IL)-10 inhibits RANTES-, tumour necrosis factor (TNF)- and nerve growth factor (NGF)-induced mast cell migratory response but is not a mast cell chemoattractant. Immunology Letters 2009;123(1):46–51. [PubMed: 19428551]
34. Reimold AM. New indications for treatment of chronic inflammation by TNF-alpha blockade. The American Journal of the Medical Sciences 2003;325(2):75–92. [PubMed: 12589232]
35. Dinarello CA. Proinflammatory Cytokines. Chest 2000;118(2):503–508. [PubMed: 10936147]

36. Anderson JM, Rodriguez A, Chang DT. Foreign body reaction to biomaterials. Semin Immunol 2008;20(2):86–100. [PubMed: 18162407]
37. Thevenot P, Hu W, Tang L. Surface chemistry influences implant biocompatibility. Curr Top Med Chem 2008;8(4):270–280. [PubMed: 18393890]
38. Wynn TA. Cellular and molecular mechanisms of fibrosis. The Journal of Pathology 2008;214(2): 199–210. [PubMed: 18161745]
39. Landgraeber S, von Knoch M, Löer F, Wegner A, Tsokos M, Huβmann B, et al. Extrinsic and intrinsic pathways of apoptosis in aseptic loosening after total hip replacement. Biomaterials 29(24–25):3444–3450. [PubMed: 18490052]
40. Hohlbaum AM, Saff RR, Marshak-Rothstein A. Fas-Ligand--Iron Fist or Achilles' Heel? Clinical Immunology 2002;103(1):1–6. [PubMed: 11987979]
41. Xie, Yanshuang; Gao, Kai; Häkkinen, Lari; Larjava, Hannu S. Mice lacking β6 integrin in skin show accelerated wound repair in dexamethasone impaired wound healing model. Wound Repair and Regeneration 2009;17(3):326–339. [PubMed: 19660040]
42. Jin DK, Shido K, Kopp HG, Petit I, Shmelkov SV, Young LM, et al. Cytokine-mediated deployment of SDF-1 induces revascularization through recruitment of CXCR4+ hemangiocytes. Nat Med 2006;12(5):557–567. [PubMed: 16648859]
43. Stellos K, Langer H, Daub K, Schoenberger T, Gauss A, Geisler T, et al. Platelet-derived stromal cell-derived factor-1 regulates adhesion and promotes differentiation of human CD34+ cells to endothelial progenitor cells. Circulation 2008;117(2):206–215. [PubMed: 18086932]
44. Chen L, Tredget EE, Wu PY, Wu Y. Paracrine factors of mesenchymal stem cells recruit macrophages and endothelial lineage cells and enhance wound healing. PLoS ONE 2008;3(4):e1886. [PubMed: 18382669]
45. Hosseinkhani H, Hosseinkhani M, Khademhosseini A, Kobayashi H, Tabata Y. Enhanced angiogenesis through controlled release of basic fibroblast growth factor from peptide amphiphile for tissue regeneration. Biomaterials 2006;27(34):5836–5844. [PubMed: 16930687]
46. Hao X, Silva EA, Mansson-Broberg A, Grinnemo K-H, Siddiqui AJ, Dellgren G, et al. Angiogenic effects of sequential release of VEGF-A165 and PDGF-BB with alginate hydrogels after myocardial infarction. Cardiovasc Res 2007;75(1):178–185. [PubMed: 17481597]
47. Sales VL, Engelmayr GC Jr, Mettler BA, Johnson JA Jr, Sacks MS, Mayer JE Jr. Transforming growth factor-beta1 modulates extracellular matrix production, proliferation, and apoptosis of endothelial progenitor cells in tissue-engineering scaffolds. Circulation 2006;114(1 Suppl):I193–199. [PubMed: 16820571]

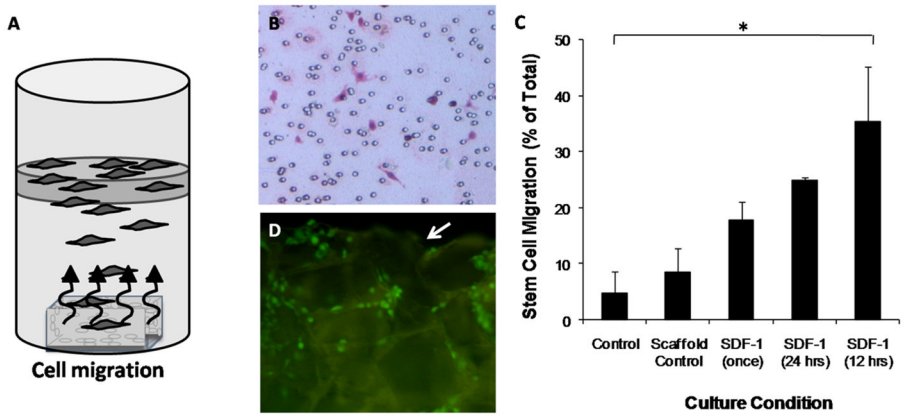

Figure 1.

Stem cell chemokine (SDF-1α) treatment induces site directed migration of primary bone marrow MSC to PLGA salt-leached scaffolds. A transwell migration in vitro model was setup to analyze the ability of SDF-1α to induce site-directed recruitment to PLGA scaffolds in vitro (A). Five conditions were tested, control (no factor or scaffold), scaffold control (scaffold only), SDF-1α supplied once at 100ng/ml, supplied every 24hrs, and supplied every 12 hrs. MSC migration across transmembranes was quantified after 48hrs by removing cells from the seeded side and H&E staining cells on the underside (B). SDF-1α induces migration of MSC across the membrane in comparison to untreated scaffolds, and additional delivery of SDF-1α increases these responses (C). Additionally, MSC transverse the membrane and migrate (CFDA-SE stained cells) onto the scaffold surface (D), with the edge of the scaffold designated by arrow (↓).

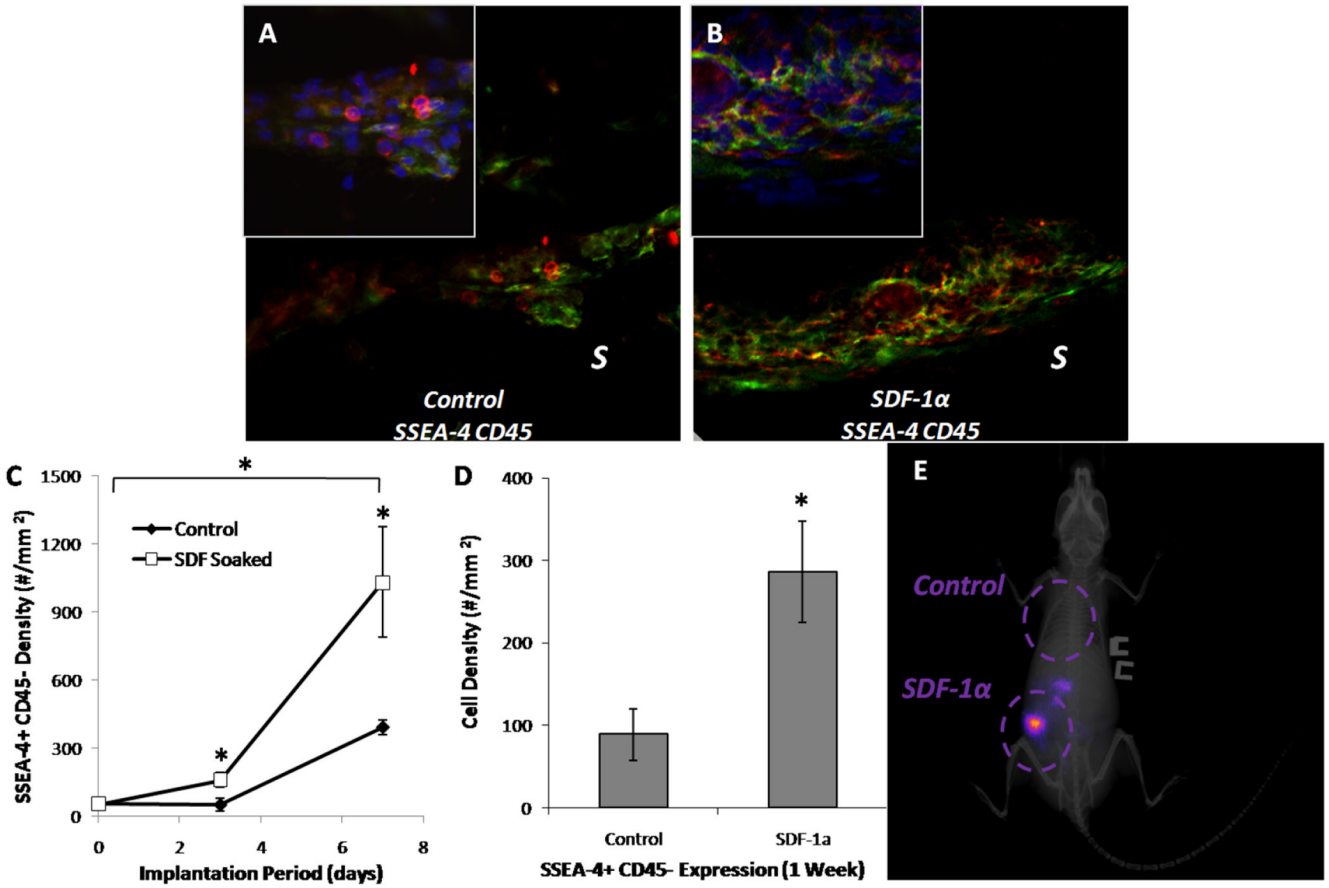

Figure 2.

SDF-1α increases engraftment of MSC (SSEA-4+ CD45− cells) to subcutaneously implanted PLGA scaffolds (SSEA-4 green, CD45 red). At Day 7, control untreated PLGA scaffolds have very low engraftment of MSC (A) while SDF-1α treated scaffolds have enhanced MSC engraftment (B). "S" indicates location of the scaffold implants. The density of engrafted MSC was quantified at Days 3 & 7 and compared between treatment groups (C). At both time points, we observe a significant, roughly 3-fold increase in engrafted MSC in the SDF-1α scaffold group, Bonferroni test ($P < 0.05$). The density of MSC in the scaffold interior was also quantified between groups (D), and reveals again a roughly 3-fold increase in MSC density, Student t-test ($P < 0.05$). SDF-1α induced engraftment of tail vein injected MSC to the site of scaffold implantation 48hrs after injection was visualized using an animal whole body imaging system (E).

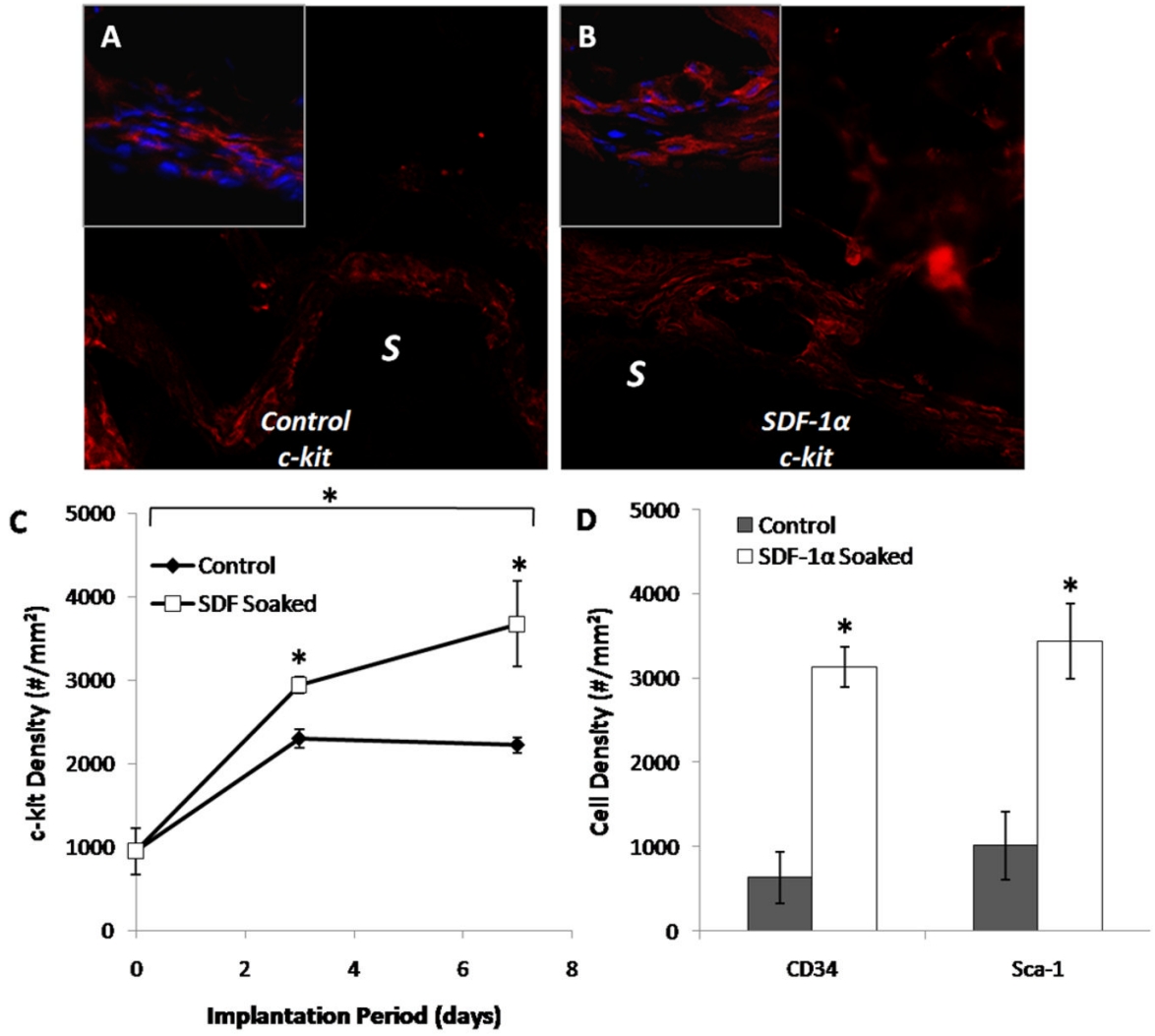

Figure 3.

SDF-1α increases HSC (c-kit+ cells) mobilization in the cellular response to subcutanesly implanted PLGA scaffolds. The density of c-kit+ cells (stained red with DAPI blue nucleus stain) near control untreated implants (A) is lower than SDF-1α scaffolds (B). "S" indicates location of the scaffold implants. The density of c-kit^{+} cells was quantified at Day 3 & 7 to compare responses between treatment groups (C). We observe significant increase in the density of c-kit+ cells at both time points, Bonferroni test ($P < 0.05$). To further characterize the HSC response, the densities of CD34+ cells as well as Sca-1+ between control and SDF-1α treated scaffolds were monitored and both are significantly elevated in the SDF-1α group (D), Student t-test ($P < 0.05$).

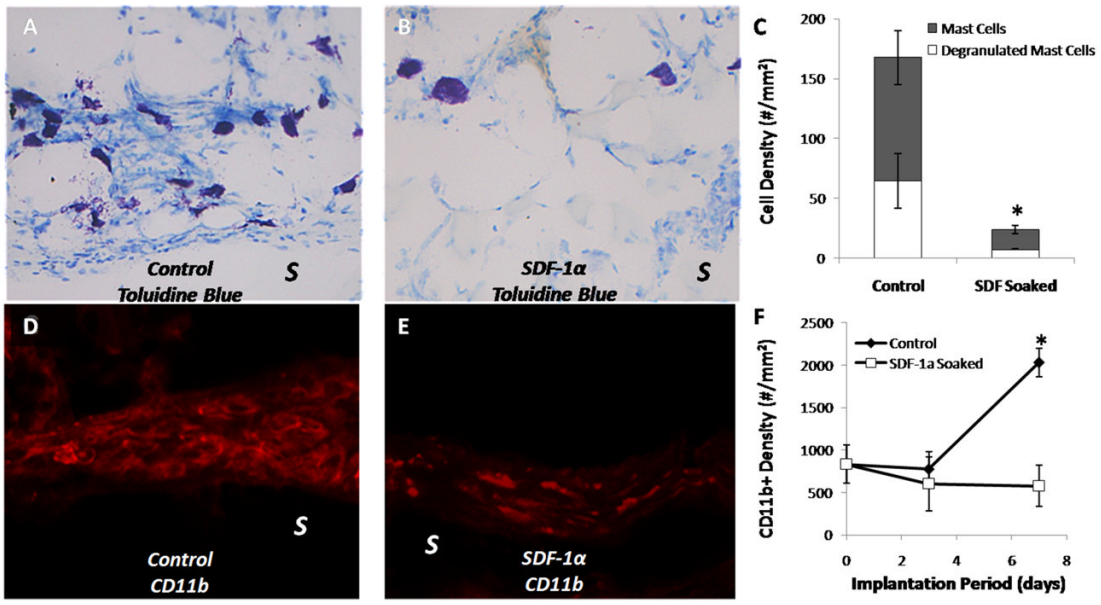

Figure 4.

SDF-1α:stem cell interactions alter mast cell responses and inflammatory cell responses during the acute inflammatory response. Mast cell responses were monitored with Toluidine Blue staining. Control scaffolds have a more prominent mast cell response (A) with several degranulated mast cells present. In contrast, SDF-1α loaded scaffolds have far fewer mast cells with little degranulation (B). "S" indicates location of the scaffold implants The density of total and degranulated mast cells was quantified and revealed significant decrease in mast cell responses in SDF-1α scaffolds (C), Student t-test ($P < 0.05$). Inflammatory cell responses were monitored by examining CD11b+ expression. Control scaffolds have thick, dense bands of CD11b+ cells (red) (D) while SDF-1α scaffolds have a lesser inflammatory response in comparison (E). Arrow (↓) designates scaffold side of the interface. The density of CD11b+ cells was quantified at Days 3 & 7 and compared between treatment groups (F), revealing a substantial decrease in cell density in SDF-1α scaffolds after Day 3, Bonferonni test ($P < 0.05$).

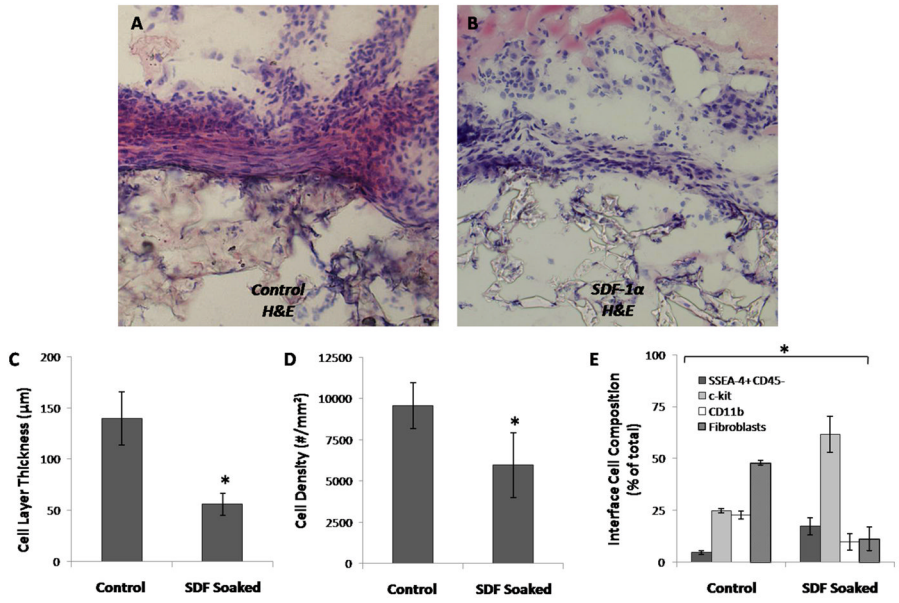

Figure 5.

Localized SDF-1α release alters the tissue response to scaffold implants and influences cellular composition at the tissue interface. The histological appearance (H&E stain) of the cell response reveals a substantial accumulation of cells at the interface of control scaffolds (A), with a much lower density evident in SDF-1α treated scaffolds (B). The thickness of the cell layer (C) and the density of cells in the response region (D) were quantified at Day 7 and compared between groups, revealing significant decreases in the SDF-1α group for both parameters, Student t-test ($P < 0.05$). Based on the quantified cell density in H&E images, the population MSC (SSEA-4+ CD45−), HSC (c-kit+ cells), inflammatory cells (CD11b+), and fibroblasts (spindle shaped cells residing near the implant interface which do not stain positive for the aforementioned markers) were plotted, revealing substantial alteration in the cell composition between treatment groups (E), Student t-test between cell grouping ($P < 0.05$ as labeled with bracket and asterisk).

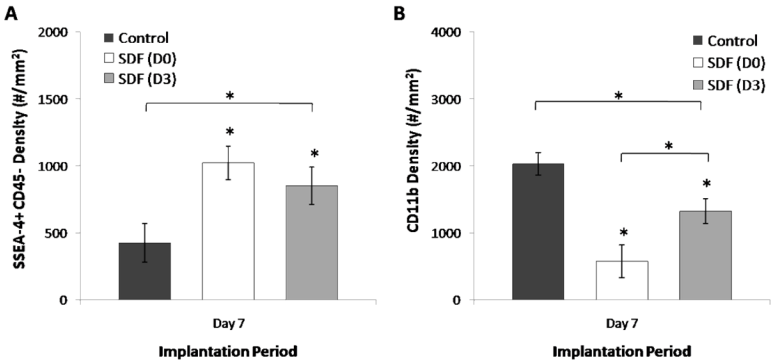

Figure 6.

SDF-1α imparts time and duration dependent alterations in the stem cell and inflammatory cell responses. Single injection at Day 3 following implantation (D3) results in an intermediate level of MSC (SSEA-4$^+$ CD45−) cells (A) between no treatment and pre-implantation SDF-1α treatment (D0). Brackets represent significant ANOVA ($P<0.05$) with (*) indicating significant Dunnett's test ($P<0.05$). The density of CD11b$^+$ cells (B) also assumes an intermediate value between no treatment and pre-treatment with SDF-1α. Brackets represent significant ANOVA ($P<0.05$) with (*) indicating significant Bonferoni test ($P<0.05$), intergroup brackets represent significance between SDF-1α treatment intervals ($P<0.05$).

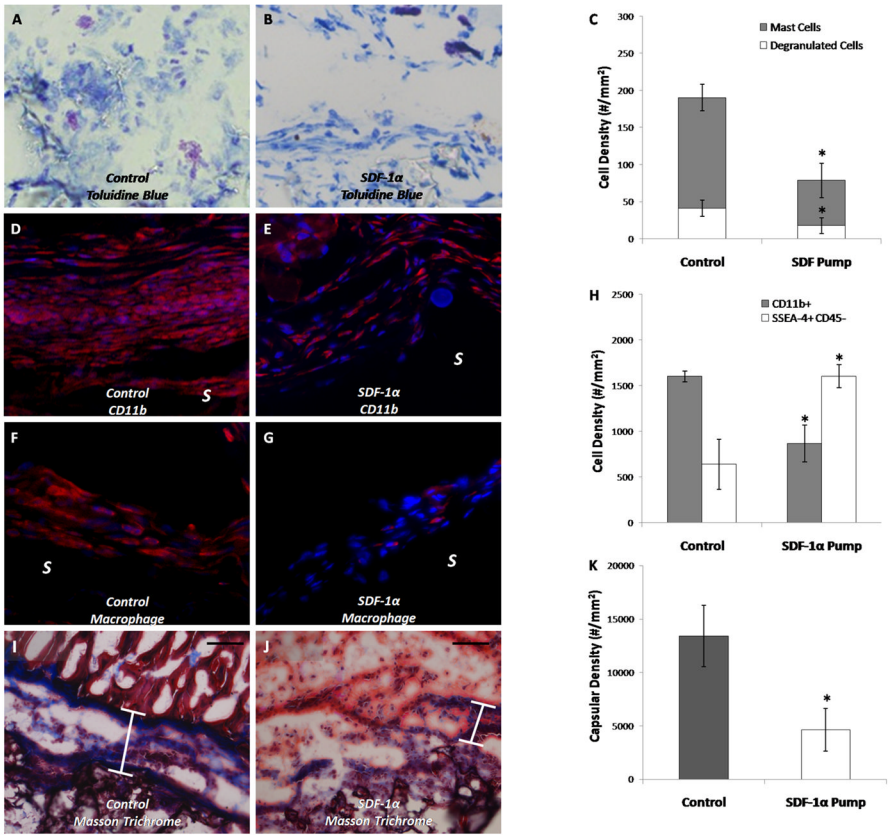

Figure 7.

Two week SDF-1α delivery modifies interface inflammatory and stem cell response. Determination of mast cell responses with Toluidine Blue again shows a more pronounced response in control group (A) in comparison to SDF-1α group (B). Quantification shows significantly more total and degranulated mast cells in control scaffolds compared to SDF-1α pump scaffolds (C). The densities of $CD11b^+$ cells were more prominent in control scaffolds (D) than SDF-1α group (E). Arrow (↓) designates scaffold side of the interface. In addition, staining for macrophage also revealed a similar trend between control (F) and treatment group (G). "S" indicates location of the scaffold implants Based on the unique response of inflammatory ($CD11b^+$) cells and MSC, we quantified and plotted the two cell populations in SDF-1α pump scaffold experiments (H). Interestingly, we observe an inversion of the two cell populations with SDF-1α treatment, with SDF-1α resulting in increased MSC density accompanied by a decrease in inflammatory cell density. Collagen deposition was monitored with Masson Trichrome staining and reveals a higher degree of deposition in control implants (I) compared to treatment group (J), brackets estimate thickness of collagen layer with scale bar (upper right corner) at 100μm. Quantification of the density (K) of cells at the interface highlights the significant difference between responses based on treatment condition. (*) significant t-test between treatment groups ($P<0.05$).

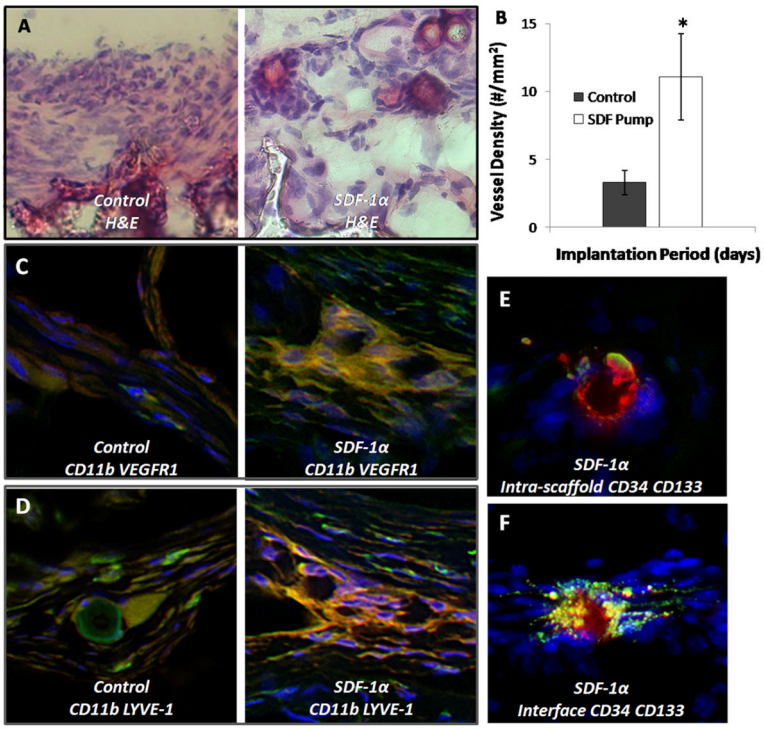

Figure 8.

SDF-1α treatment improves EPC engraftment and participation of macrophage subsets in angiogenesis and lymphangiogenesis. H&E staining was used to examine the cellular response at the interface. Control scaffolds have a thick, dense cellular response (A) at the interface while SDF-1α group has a weaker cell response with the appearance of budding vessels at the interface. Quantification of vessel density within the scaffold implants reveals a significant difference in the degree of vessel formation (B), Student t-test ($P < 0.05$). Control scaffolds also have few cells co-expressing CD11b (green) and VEGFR1 (red) (C) in agreement with a low number of budding vessels. However, we do find the groups of cells expressing these markers in SDF-1α scaffolds. Control scaffolds have few cells staining positive for CD11b (green) LYVE-1 (red) (D) which are involved in lymphogenesis, while SDF-1α have organized groups of cells staining positive. The presence of EPC cells inside the scaffold (E) and at the interface (F) of SDF-1α modified scaffolds was monitored by expression of $CD34^+$ (green) $CD133^+$ (red) markers.

Table 1

SDF-1α release and stem cell responses alter the cytokine/chemokine environment at 2 weeks. Inflammatory protein arrays were used to quantify the presence of different proteins in the implant sections. SDF-1α scaffold values were compared to controls and tabulated as fold increase (left column) or fold decrease (right column – underlined).

	Expression			Expression	
Protein	**Increase**	**Decrease**	**Protein**	**Increase**	**Decrease**
Axl	1.20		IL-9		5.21
BLC/CXCL13	1.55		KC/CXCL1	8.56	
CD30 L		2.62	Leptin		1.80
CD30 T		1.57	Leptin R/CD295		4.26
CD40		2.15	LIX/CXCL5		1.07
CRG-2/CXCL10		2.70	L-Selectin/CD62L		2.08
CTACK/CCL27		2.25	Lymphotactin/XCL1		3.26
CXCL16	2.80		**MCP1**/CCL2	1.80	
Eotaxin/CCL11	2.01		**MCP-5**/CCL12		1.45
Eotaxin-2/CCL24		2.03	**M-**CSF		1.41
Fas Ligand/CD95L		3.98	**MIG**/CXCL9	1.32	
Fractalkine		1.49	**MIP-1α**/CCL3	24.39	
GCSF	81.90		**MIP-1γ**/CCL9	1.29	
GM-CSF	49.57		**MIP-2**/CXCL2	120.63	
IFNγ		1.70	**MIP-3 β**/CCL20		2.14
IGFBP-3	6.01		**MIP-3α**/CCL19		2.67
IGFBP-5		1.22	**PF-4**/CXCL4	7.06	
IGFBP-6		1.99	P-Selectin/CD62P		1.12
IL-1β		1.20	**RANTES**/CCL5	1.76	
IL-10		2.12	SCF/CD117		1.74
IL-12 p40/p70	3.33		**SDF-lα**/CXCL12		1.39
IL-12 p70		1.74	**sTNF RI**/CD120a		1.14
IL-13		5.02	**sTNF RII**/CD120b	2.91	
IL-17	1.47		**TARC**/CCL17	3.41	
IL-1α		1.18	**TCA-3**/CCL1		4.27
IL-2		1.71	**TECK**/CCL25		1.07

Protein	Expression		Protein	Expression	
	Increase	Decrease		Increase	Decrease
IL-3		1.91	**TIMP-1**	2.05	
IL-3 Rβ		2.74	**TNFα**		2.57
IL-4		2.14	**TPO**		1.24
IL-5		3.46	**VCAM-1/CD106**	1.13	
IL-6	13.54		**VEGF**	2.93	